Photo 1. One stop center in Chungliao, Sep. 1999.

Photo 2. Relief goods in Chungliao, Sep. 1999.

Photo 3. Surface fault break in Wufeng, Sep. 1999.

Photo 4. Slope failure in Kouhsing, Sep. 1999.

Photo 5. Collapse of high-rise RC buildings in Taichung City, Sep. 1999.

Photo 6. Collapse of high-rise RC buildings in Tali, Sep. 1999.

Photo 7. Collapse of 2-4-story RC buildings in Fengyuan, Sep. 1999.

Photo 8. Collapse of 2-4-story RC buildings in Chungliao, Sep. 1999.

Photo 9. Inclined RC building just on the fault rupture in Fengyuan, Sep. 1999.

Photo 10. Collapsed buildings due to the surface faulting in Wufeng, Sep. 1999.

Photo 11. Damages of low-rise non-engineered buildings constructed during Japanese occupation era in Chi-Chi, Sep. 19999.

Photo 12. Inclined building in Yuanlin district, Oct. 1999.

Photo 13. Collapsed Pi-feng Bridge in Fengyuan, Sep. 1999.

Photo 14. Collapsed Chang-gang Bridge in Shihkang, Sep. 1999.

Photo 15. Damaged Shih-kang Dam in Shihkang, Sep. 1999.

Photo 16. Damaged buried pipelines in Takeng district, Taichung City, Sep. 1999.

Photo 17. Inclination of telegraph poles and ground deviations at waterway in Yuanlin district, Oct. 1999.

Photo 18. Ground depressions at North terminal in Taichung Harbor, Oct. 1999.

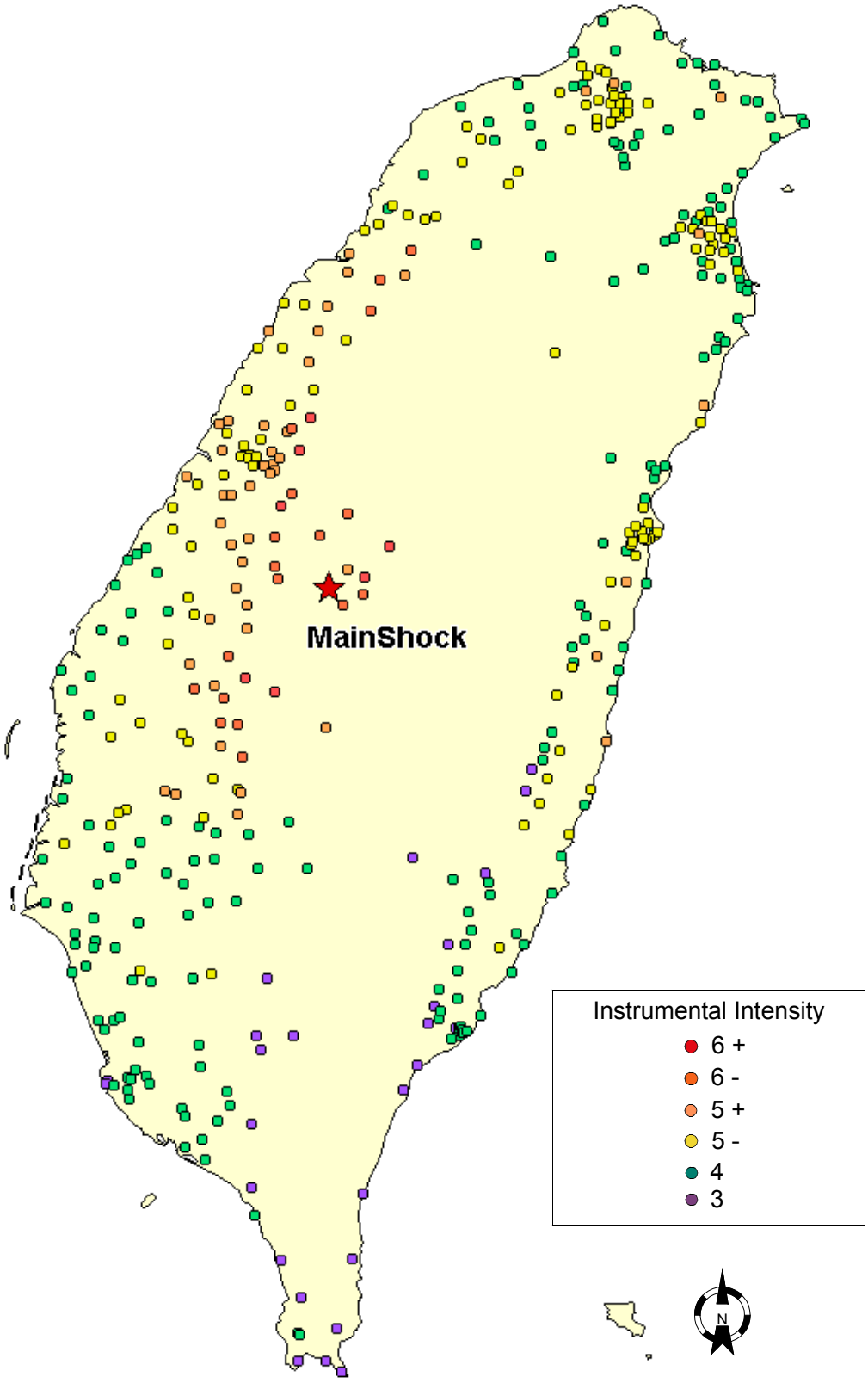

Figure 1. Distribution of the JMA seismic intensity for the 1999 Chi-Chi earthquake (Refer to Section 2.2).

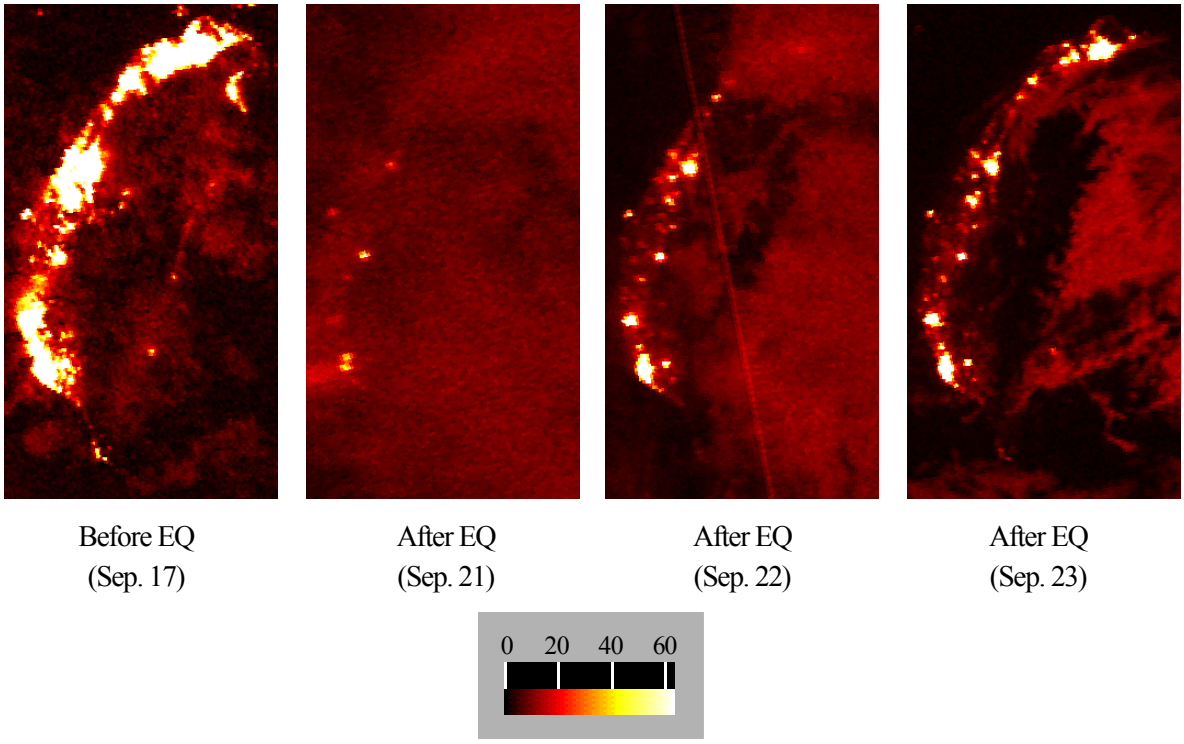

Figure 2. VNIR images before and after the earthquake (Refer to Section3.1).

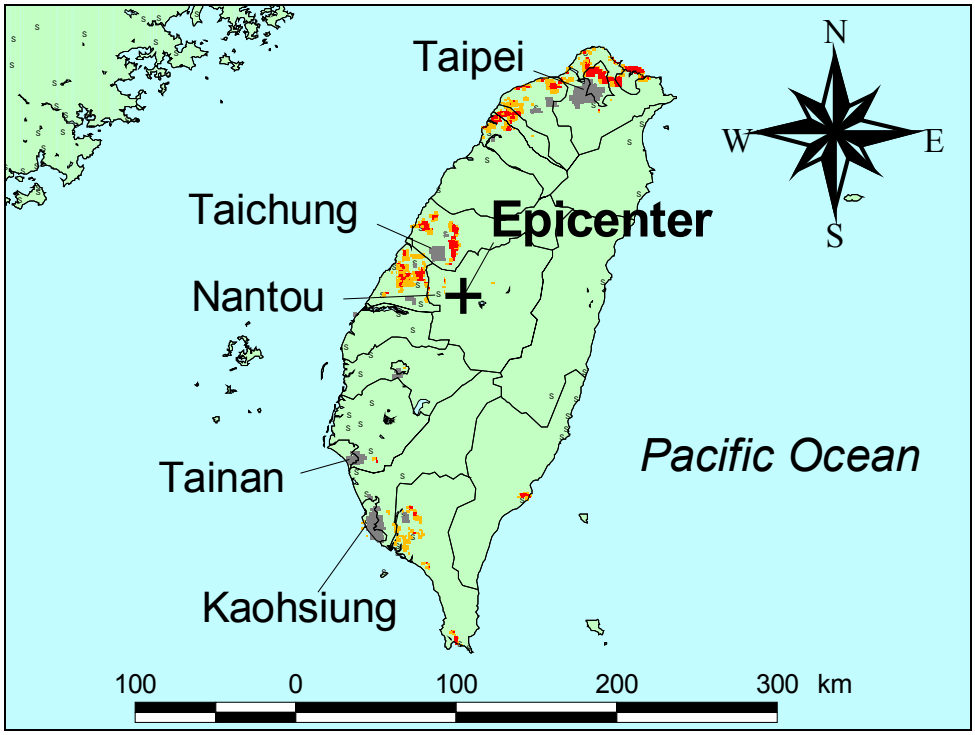

Red: possible impacted areas ($p > 97.5\%$), Yellow: possible impacted areas ($p > 95\%$)
Gray: incapable of estimation due to saturated data

Figure 3. Estimated damaged areas of the 1999 Chi-Chi Earthquake, Taiwan (Refer to Section3.1).

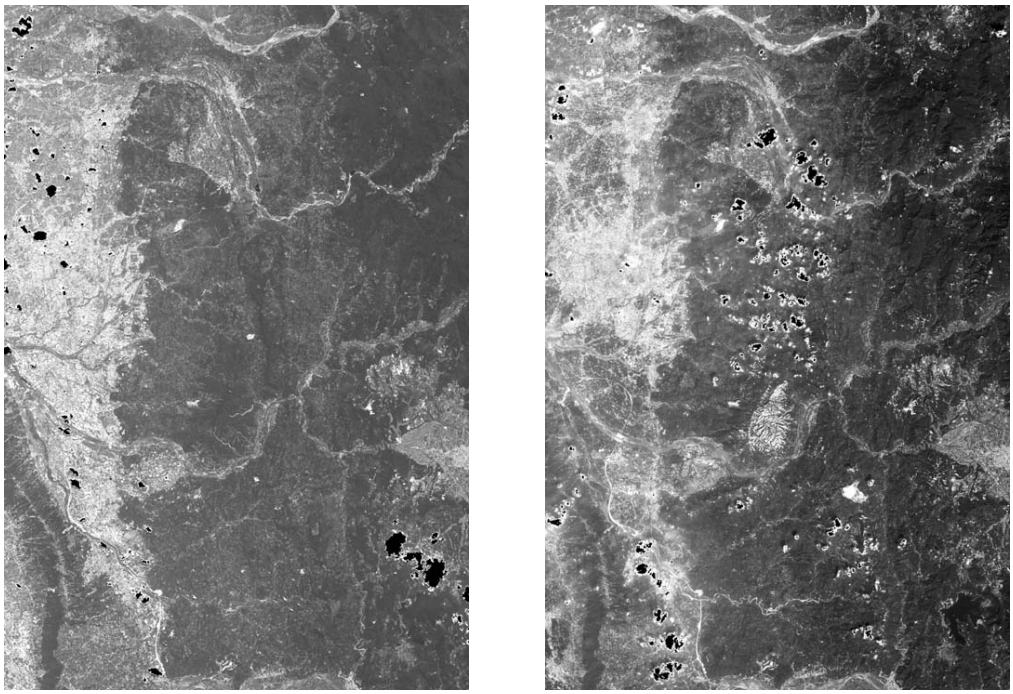

(a) Image taken on 06/24/99 (b) Image taken on 09/27/99

Figure 4. SPOT/HRV panchromatic images of the strongly affected area by the Chi-Chi earthquake; Black areas indicate masking by clouds (Refer to Section 4.1).

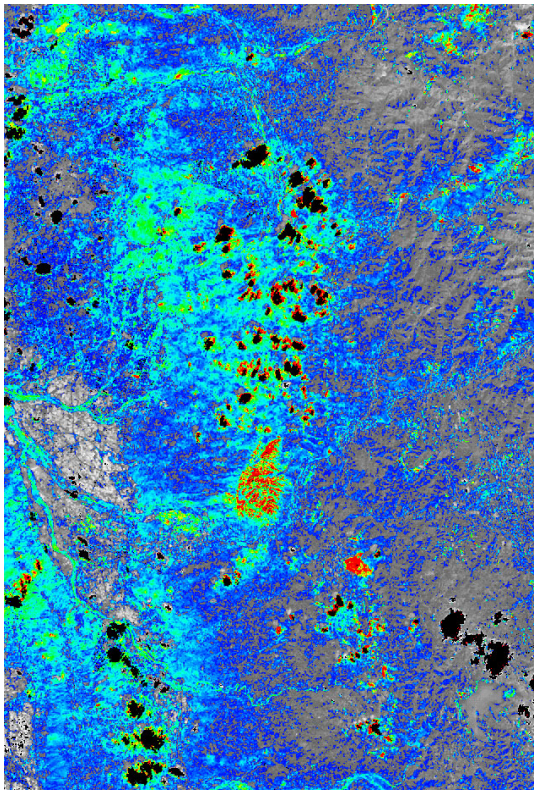

Figure 5. Pseudo color image of *ND* values overlaid on the pre-event panchromatic image. Red color may correspond to slope failures and landslides (Refer to Section 4.1).

(a) Aerial HDTV image

(b) Building damage distribution obtained by the automated detection

(c) Building damage distribution obtained by the visual inspection

Figure 6. Building damage detection based on aerial HDTV image for Chungliao area (Refer to Section 4.2).

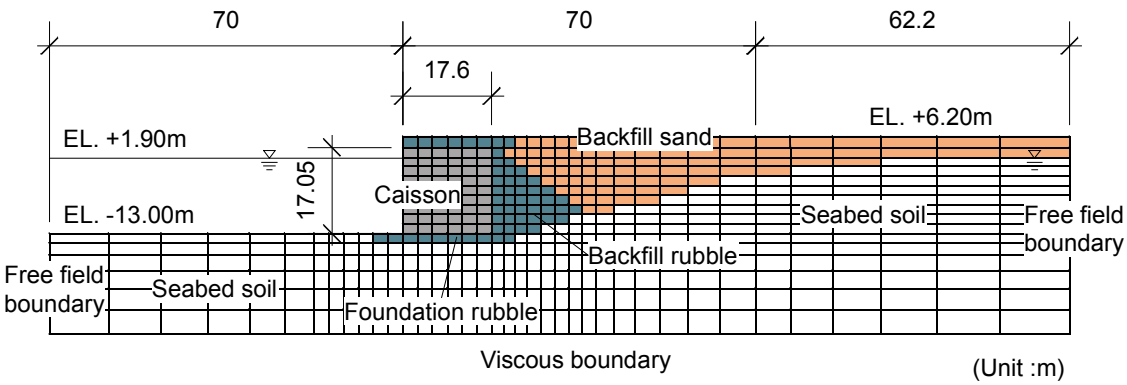

Figure 7. FE model for Pier No.2 of Taichung Harbor (Refer to Section 5.1).

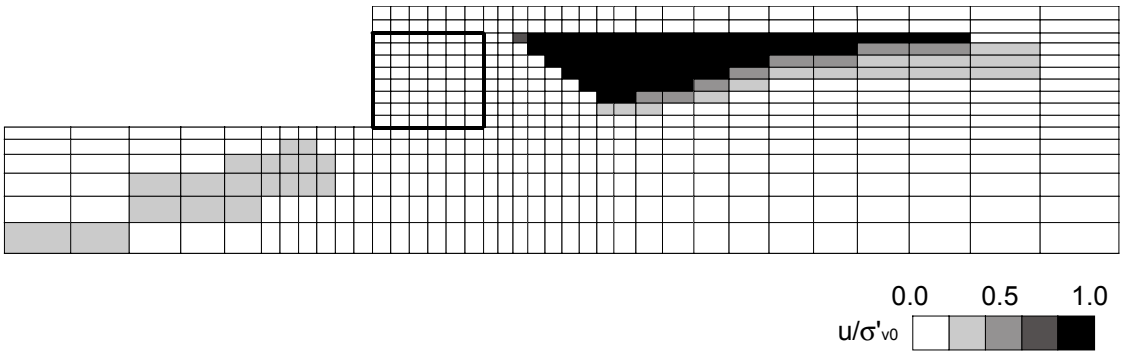

(a) Distribution of excess pore water pressure ratio

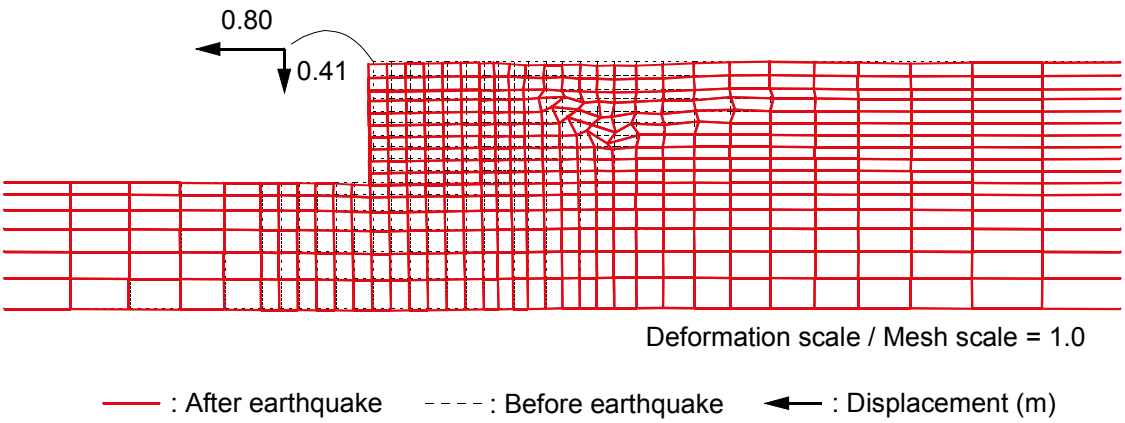

(b) Deformed configuration after earthquake

Figure 8. Numerical results by effective stress analysis (Refer to Section 5.1).